

Microstructure and electroluminescence of ZnS:Cu,Cl phosphor powders prepared by firing with CuS nanocrystallites

Yung-Tang Nien · In-Gann Chen ·
Chii-Shyang Hwang · Sheng-Yuan Chu

Received: 26 June 2005 / Revised: 31 October 2005 / Accepted: 24 April 2006
© Springer Science + Business Media, LLC 2006

Abstract This paper presents the microstructure and electroluminescent performance of ZnS:Cu,Cl phosphor powders prepared by firing micrometer-sized ZnS with NaCl and CuS nanocrystallites at 900°C in the reducing atmosphere. A series of samples with Cu addition ranging from 40 to 5000 ppm were studied. XRD analysis showed that ZnS:Cu,Cl samples with Cu addition of ≥ 400 ppm exhibited a transformation from hexagonal to cubic structure. The whole series of ZnS:Cu,Cl samples showed significant photoluminescent (PL) intensity; however, only samples with Cu addition of ≥ 400 ppm revealed measurable electroluminescent (EL) intensity. This difference was supposed to be a result of nano-sized Cu_xS precipitation in ZnS during firing treatment, where Cu_xS acted as electron emission source to enhance the EL intensity. Furthermore, ZnS:Cu,Cl powder sections were analyzed using X-ray mapping (XRM) of a scanning transmission electron microscope, revealing that Cu_xS precipitates of 50–80 nm in size were observed only in the samples with EL emission, i.e. Cu addition ≥ 400 ppm. The variation of EL intensity was interpreted in terms of the concentration of Cu activators as well as the phase and the amount of Cu_xS in ZnS.

Keywords Electroluminescence · ZnS · Precipitate · Ultramicrotomy · X-ray mapping

Y.-T. Nien · I.-G. Chen (✉) · C.-S. Hwang
Department of Materials Science and Engineering, National Cheng-Kung University, Tainan, Taiwan
e-mail: ingann@mail.ncku.edu.tw

S.-Y. Chu
Department of Electrical Engineering, National Cheng-Kung University, Tainan, Taiwan

Introduction

Zinc sulfide (ZnS) is a semiconductor material with bandgap energies of 3.7 and 3.8 eV in zinc blende and wurtzite structure, respectively [1]. Due to its excellent electrical properties such as the large band-gap energy, direct recombination and high resistance to electric field, ZnS has great potential of being used as solar cells [2], infrared windows [3], and phosphor materials by doping with transition or rare-earth metals [4, 5]. In addition, owing to the advantages of the simple manufacturing process, the convenience of being able to print large area and the high power efficiency, ZnS electroluminescent (EL) phosphor powders would be suitable for back lighting of liquid crystal panels or for flat panel displays.

The most widely used EL phosphor material is ZnS:Cu,Cl in which Cu behaves as an acceptor contributing to the emission, and Cl behaves as a donor. In this study, micrometer-sized ZnS powders were fired with NaCl and various amount of CuS nanocrystallites to study the EL performance. Experimental data indicated that the crystal structure and the EL intensity of ZnS:Cu,Cl depended on the amount of Cu addition. EL was observed only in the cubic structure of ZnS powders with Cu addition of ≥ 400 ppm. The variation of EL intensity will be interpreted in terms of the concentration of Cu activators as well as the phase and the amount of Cu_xS precipitates in ZnS.

Experimental procedure

Luminescence grade ZnS powders (99.99%, $< 10 \mu\text{m}$, Acros) were mixed with 1 wt.% NaCl (99.5%, Showa) and 40–5000 ppm CuS nanocrystallites in alcohol, where CuS nanocrystallites were synthesized by co-precipitation of $\text{CuCl}_2 \cdot 2\text{H}_2\text{O}$ (99%, Showa) and $\text{Na}_2\text{S} \cdot 9\text{H}_2\text{O}$ (98%, Showa)

solutions. The mixed powders were dried in the oven at 80°C and then fired in the tubular furnace at 900–1050°C for 2 h in the mixed atmosphere of 3%H₂/Ar and sulfur. Finally, the ZnS:Cu,Cl powders were washed with ammonium hydroxide (29.7%, J.T. Baker) to remove the residual copper sulfides.

An X-ray diffractometer with Cu K α radiation (XRD, D/max, Riguka) was employed to characterize the crystal structure of ZnS:Cu,Cl powders with various amount of Cu addition. The photoluminescence (PL) of ZnS:Cu,Cl powders was carried out using a Xe lamp with an excitation wavelength of 343 nm. For EL measurement, the ZnS:Cu,Cl powders were mixed in castor oil as dispersion media, followed by being injected into a cell of indium tin oxide(ITO)-coated glass and Al sheet with a space of 80 μ m. The weight ratio of ZnS:Cu,Cl powders to castor oil was 1/6. The EL cell of 15 \times 15 mm² in area was excited with an alternating current bias voltage of 300 V and frequency of 1 kHz. The PL and EL were examined using optic fibers and an optical detector with CCD arrays (Model USB2000, Ocean Optics) at room temperature under ambient atmosphere.

The ZnS:Cu,Cl powders with a particle size of 2–5 μ m were embedded in an epoxy-resin mount (Embed-812, EMS) to help retain the shape for sectioning by an ultramicrotome (Ultracut E, Reicher-Jung). A diamond knife with an angle of 35° (ultra, Diatome) was used to cut ZnS:Cu,Cl powders. The cut sections were put onto carbon-coated Au sample grids. The sectioning procedure has been outlined by Mails and Steele [6]. The microstructure and chemistry of sections were analyzed on a Be double tilt sample holder using a scanning transmission electron microscope (STEM, JEM-2100F, JEOL) equipped with an energy dispersive spectrometer (EDS, Link-ISIS, Oxford) operated at 200 kV. For EDS microanalysis, the spot size of electron beam was 0.7–1.5 nm with a dwell time of 25–50 ms in order to permit enough X-rays to be generated and collected from this reduced interaction volume.

Results and discussion

Structure analysis of ZnS powders with various amount of Cu addition after being fired at 900°C for 2 h was carried out by the X-ray powder diffraction method. It is known that ZnS crystallizes either as a cubic structure (zinc blende or β -ZnS) or as a hexagonal structure (wurtzite or α -ZnS). The β -ZnS structure corresponds to the low temperature phase, and then transforms to α -ZnS at approximately 1020°C [1, 7]. The XRD spectra in Fig. 1(a)–(e) show that α -ZnS and β -ZnS coexisted in the ZnS:Cu,Cl powders with Cu addition of 40, 80, 120, 200 and 400 ppm, respectively. In Fig. 1(e) and (f), a decrease of (100) $_{\alpha}$ and (101) $_{\alpha}$ peak intensities can be observed, which illustrates that α -ZnS decreased and β -

ZnS increased in the samples with increasing Cu addition. Moreover, in the samples with Cu addition of >800 ppm, α -ZnS was less observed as revealed in Fig. 1(g)–(j).

By using the absolute standard method [8, 9], the weight ratio of α -ZnS to β -ZnS (W_{α}/W_{β}) could be determined by calculating the integrated intensity ratio of $I_{(100)\alpha}$ to $I_{(200)\beta}$ diffraction peaks with a factor of 0.0968 as follows:

$$W_{\alpha}/W_{\beta} = 0.0968[I_{(100)\alpha}/I_{(200)\beta}] \quad (1)$$

$$Hexa\% = [W_{\alpha}/(W_{\alpha} + W_{\beta})] \times 100\% \quad (2)$$

The (100) $_{\alpha}$ and (200) $_{\beta}$ peaks were chosen due to their strong reflection without overlapping the peaks of another phase. Figure 2 shows the weight ratio of α -ZnS to β -ZnS in ZnS:Cu,Cl powders with different amount of Cu addition. The curve (a) in Fig. 2 shows that under a firing temperature of 900°C for 2 h, there was around 30 and 18 wt.% α -ZnS (*Hexa*%) formed in the samples with Cu addition of 40–200 and 400 ppm, respectively. However, β -ZnS dominated in the samples with Cu addition of \geq 400 ppm. It has been reported that the Cu addition in excess of its solubility limit in ZnS would precipitate to form a second phase of Cu_xS, which would then initiate the β -ZnS transformation [10, 11]. Therefore, the samples with Cu addition of <400 ppm were predicted to be free from precipitates, while those with Cu addition of \geq 400 ppm would have different amount of precipitates depending on the amount of Cu addition. A series of ZnS:Cu,Cl powders were also fired at a higher temperature of 1050°C for 2 h in order to validate the previous statement. The weight ratio of α -ZnS to β -ZnS fired at 1050°C estimated from the XRD spectra (not shown here) is presented as curve (b) in Fig. 2. This indicates that a higher fraction of β -ZnS was transformed to α -ZnS (~80 wt.%) in the samples with Cu addition of 40–200 ppm in comparison to those fired at 900°C (~30 wt.%). It can also be found from curve (b) that the samples with Cu addition of >200 ppm were nearly all β -ZnS phase. According to the results shown above, we can predict that the solubility limit of Cu in α -ZnS was 800 and 400 ppm when fired at 900 and 1050°C, respectively. It should be noted that there was less α -ZnS in the sample with Cu addition of 400 ppm fired at 1050°C when compared to that fired at 900°C. It is supposed to result from the enhancement of transformation by the initial precipitation at a higher temperature because of the endothermic reaction of β -ZnS transformation.

According to the bipolar field emission model proposed by Fischer [12, 13], conductive impurities such as cuprous sulfides (Cu_xS) are necessary for luminescent ZnS particles to intensify the electric field, and to allow holes and electrons to recombine with radiation in luminescent centers. Therefore, by referring to the XRD analysis shown above, we can also predict that the samples fired at 900°C with Cu

Fig. 1 XRD spectra of ZnS:Cu,Cl with Cu addition in the range of 40 to 5000 ppm fired at 900°C

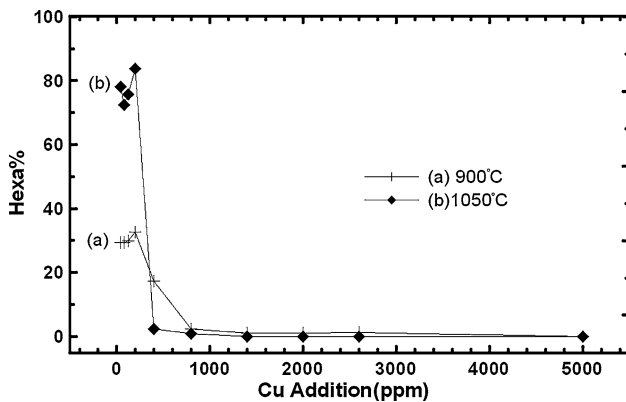
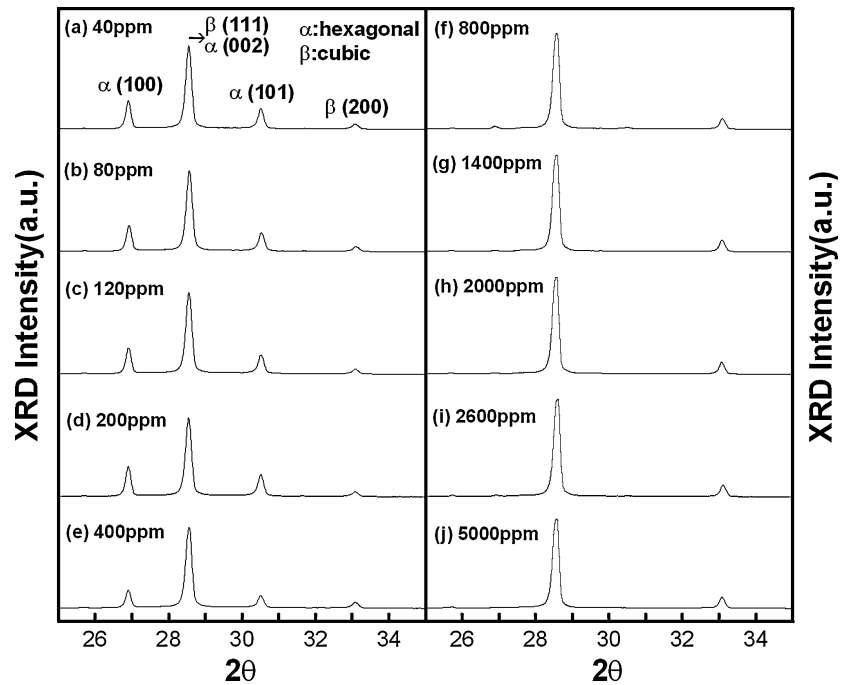


Fig. 2 The weight ratio of α -ZnS to β -ZnS in ZnS:Cu,Cl powders fired at (a) 900°C and (b) 1050°C

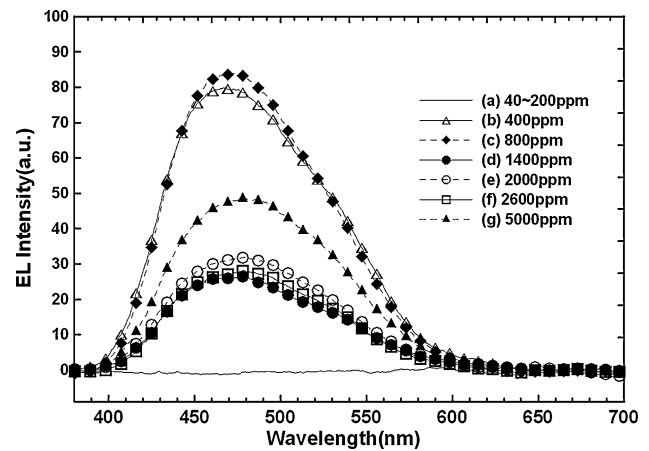


Fig. 3 EL spectra of ZnS:Cu,Cl with various amount of Cu addition fired at 900°C for 2 h in the reducing atmosphere. (Ex. 300VAC 1 kHz)

addition of 40–200 ppm would not perform EL as excited by an electric field due to the lack of Cu_xS precipitates though PL was observed in all samples. Figure 3 shows the EL emission spectra of ZnS:Cu,Cl powders with various amount of Cu addition. Exactly no significant luminescence was detected under electric field excitation in the samples with Cu addition of 40–200 ppm as shown in Fig. 3(a). However, the samples with Cu addition ranging from 400 to 5000 ppm showed EL emission under the same electric field excitation as revealed in Fig. 3(b)–(g). In Fig. 3, the EL spectra of ZnS:Cu,Cl powders showing a non-Gaussian distribution in the range of 400–600 nm were similar to that excited by cathode rays [14], yet they consisted of blue and green emission bands. This can be explained by a model provided by Kawai [15] in which the quenching of green-luminescence and the appearance of blue-luminescence were derived from the in-

terstitial Cu^+ . Therefore, it was supposed that ZnS powders with Cu addition in the range of 400–5000 ppm were doped with Cu both substitutionally and interstitially. The decrease of emission intensity with increasing Cu addition beyond 800 ppm in Fig. 3(d)–(f) is believed to result partly from the activator concentration quenching effect [15], indicating that the excess doped-Cu provides the dominant non-radiative path for excitation energy. The increased EL intensity in the sample with Cu addition of 5000 ppm is supposed to be induced by the variable electrical properties as well as the phase of Cu_xS precipitates, which will be discussed in detail later.

The ultramicrotomy technique was used to prepare STEM specimens for microanalysis because it has fewer problems

as compared to the other methods, such as electropolishing and ion beam thinning [6]. Due to the hard and brittle nature of ZnS, the thin specimens tended to fracture during the sectioning process. Nevertheless, the mechanical damage was localized, and damage-free areas were relatively large for high-resolution images and microanalysis as illustrated in Fig. 4. Figure 4(a) shows a STEM bright field image of a piece of a ZnS:Cu,Cl particle with Cu addition of 5000 ppm. The inset shown in Fig. 4(a) is the corresponding diffraction pattern in [110] zone axis, indicating the cubic structure in consistent with the XRD analysis. Figure 4(b) and (c) show the Zn and Cu characteristic X-ray mapping (XRM) images, respectively. The uniform intensity of Zn X-rays shown in Fig. 4(b) indicates very little thickness variation in the section besides the arrowed area was induced by the overlapping of section chips. Owing to the doped-Cu activators in ZnS being less than the minimum mass fraction (MMF) for EDS to detect, the Cu characteristic X-rays presented inhomogeneously in Fig. 4(c) was assumed to be radiated from Cu_xS precipitates. The Cu_xS precipitates were observed in all specimens with Cu addition of >200 ppm; however, no significant Cu characteristic X-rays were detected in the samples with Cu addition of <400 ppm. We supposed that there was no Cu_xS precipitates formed in these lower Cu added samples in agreement with the XRD and EL results. According to the Monte-Carlo simulation [16], we can derive the electron interaction volume and the X-ray source size based on the beam energy, spot size (1.5 nm) and the thickness of specimen (50–100 nm). The beam spreading radius of 3–7.5 nm was simulated using parameters of 200 kV accelerating voltage and atomic number of $Z = 29$ (Cu) in the thickness range of 50–100 nm, which was smaller than the step of scanning points (~ 8.2 nm). Therefore, the spatial resolution of microanalysis shown here was equivalent to the step size. In Fig. 4(c), the areas radiating the Cu characteristic X-rays were of approximately 50–80 nm in size, which were estimated to be the size of Cu_xS precipitates or the aggregates of precipitates.

On the basis of the previous studies [12, 13] and results shown above, EL has been attributed to the ionization of activators by the impact of charge carriers accelerated by the high electric fields between Cu_xS precipitates and ZnS:Cu,Cl matrix. It is believed that both the amount as well as the physical properties of Cu_xS precipitates would influence the recombination rate and the following EL intensity. In Fig. 3(b) and (c), the sample with Cu addition of 400 ppm showed lower EL intensity compared to that with Cu addition of 800 ppm. It would result from both a lower fraction of β -ZnS and an inadequate amount of Cu_xS precipitates for charge carriers tunneling through the Cu_xS -ZnS contact to excite activators. The decreased EL intensity in the samples with Cu addition beyond 800 ppm in Fig. 3(d)–(f) is believed to be due to the concentration quenching effect of activators and

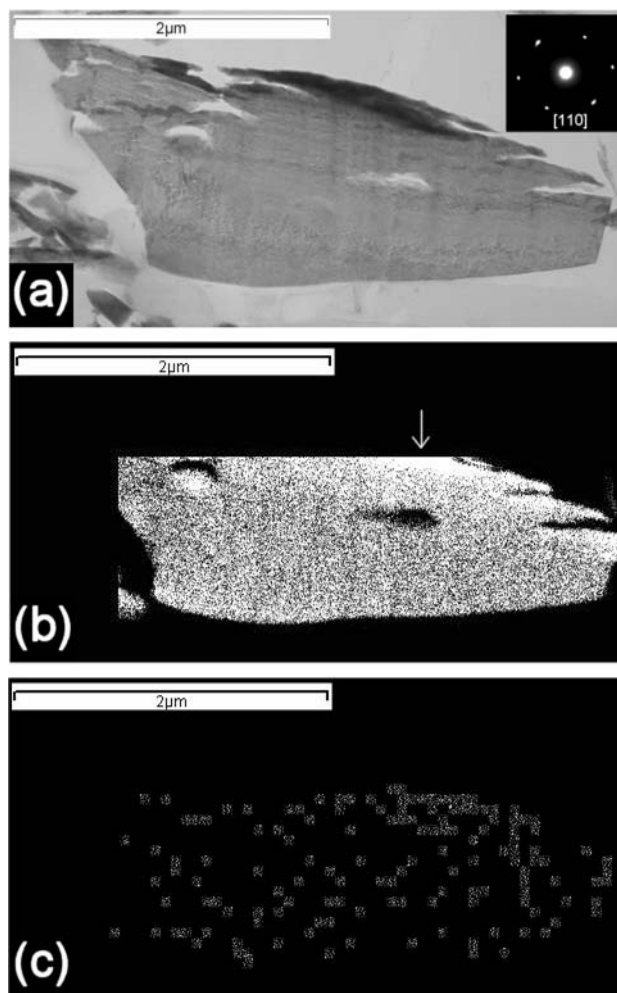


Fig. 4 (a) STEM bright field image of ZnS:Cu(5000 ppm),Cl powder section with an inset showing the cubic diffraction pattern in [110] zone axis. (b) and (c) reveal the corresponding Zn α and Cu α X-ray mapping results of the section, respectively. [The arrow in Fig. 4(b) reveals the overlapping of section chips.]

Cu_xS precipitates. An increase of Cu_xS precipitates would increase the tunneling current and also induce the inelastic scattering among tunneled charge carriers. The EL intensity would show a maximum and then begin to decrease due to the limited activators and energetic charge carriers available for excitation.

The inversed higher EL intensity in the sample with Cu addition of 5000 ppm is observed in Fig. 3(g). It is supposed to result from the polymorphism as well as the variable physical properties of Cu_xS precipitates. The copper-sulfur phase diagram is relatively complex, especially in the composition range relevant to solar cells, i.e. from Cu_2S to $\text{Cu}_{1.78}\text{S}$ [17]. The structure of Cu_xS as well as its electrical and optical properties has been found to vary with the stoichiometric value of x [18]. Nair et al. [19] reported that the resistance and the bandgap energy (E_g) of Cu_xS increase as x approaches 2. It is also known that the instantaneous field-emission or

tunneling current I through the Cu_xS -ZnS contact follows the Fowler-Nordheim equation:

$$I = A \frac{E^2}{W^{3/2}} \exp\left(-B \frac{W^{3/2}}{E}\right) \quad (3)$$

where A and B are constants, E is the field strength, and W is the work function. In this case, the work function W corresponds to the energy difference between the electron affinity of ZnS and that of Cu_xS . The lower tunneling current through the Cu_xS -ZnS contact due to the larger E_g of precipitates as well as the higher work function W would result in the adequate excitation of activators and higher EL intensity. Therefore, the ZnS:Cu,Cl powders with higher Cu addition of 5000 ppm were supposed to separate copper-rich Cu_xS precipitates with larger E_g . Further experiments to study the distribution of precipitates quantitatively and identify their stoichiometric value of x to support this hypothesis are in progress.

Conclusions

Electroluminescent ZnS:Cu,Cl phosphor powders have been prepared by firing ZnS with NaCl and CuS nanocrystallites at 900°C for 2 h. XRD analysis showed that the ZnS:Cu,Cl phosphor powders with Cu addition of <400 ppm were hexagonal structure, while the powders with Cu addition of ≥ 400 ppm were cubic. Though all ZnS:Cu,Cl powders showed PL emission, EL emission was only observed in the ZnS:Cu,Cl powders with Cu addition of ≥ 400 ppm. The microanalysis by X-ray mapping indicated that Cu_xS precipitates of 50–80 nm in size were observed only in the samples with Cu addition of ≥ 400 ppm, which were inferred to induce the phase transformation and the EL emission. The variation of EL intensity in the samples with different amount of Cu addition was related to the concentration of activators, the amount and the phase of Cu_xS precipitates. An optimal EL intensity was observed in the ZnS:Cu,Cl powders with Cu addition of 400–800 ppm. In addition to the activator concentration quenching effect, the decreased EL intensity of the ZnS:Cu,Cl powders with Cu addition beyond 800 ppm was supposed to result from the increase of inelastic scattering

of charge carriers tunneling from the excess Cu_xS precipitates. Copper-rich Cu_xS precipitates with larger E_g in the ZnS:Cu,Cl powders were inferred to induce the increased EL intensity because of the appropriate amount of charge carriers and activators.

Acknowledgments This work was supported under projects from the National Science Council (NSC 91-2622-E-006-059-CC3 and NSC-92-2622-E-006-129-CC3) of Taiwan. The author (Y.T. Nien) also thanks the Center for Micro/Nano Technology Research, National Cheng-Kung University, Taiwan, for providing student scholarship and their support in TEM sample preparation.

References

1. S. Shionoya, in *Phosphor Handbook*, edited by S. Shionoya and M. William (CRC Press, Boca Raton, 1999), p. 232.
2. T. Nakada, K. Furumi, and A. Kunioka, *IEEE Trans. Electron. Devices*, **46**, 2093 (1999).
3. A. Fujii, H. Wada, K.I. Shibata, S. Nakayama, and M. Hasegawa, in *Window and Dome Technologies and Materials VII*, edited by R.W. Tustison (SPIE, Bellingham, 2001), p. 206.
4. D.S. McClure, *J. Chem. Phys.*, **39**, 2850 (1963).
5. R.E. Shrader, S. Larach, and P.N. Yocom, *J. Appl. Phys.*, **42**, 4529 (1971).
6. T.F. Mails and D. Steele, in *Specimen Preparation for Transmission Electron Microscopy of Materials II*, edited by R.M. Anderson (Materials Research Society, Pittsburgh, 1990), p. 3.
7. E.T. Allen and J.L. Crenshaw, *Am. J. Sci.*, **34**, 341 (1912).
8. B.D. Cullity and S.R. Stock, *Elements of X-ray Diffraction* (Prentice-Hall, New Jersey, 2001) p. 347.
9. B.L. Li, C.X. Guo, and Y.T. Wan, *Acta Physica Sinica*, **40**, 490 (1991).
10. J. Nickerson, P. Goldberg, and D.H. Baird, *J. Electrochem. Soc.*, **110**, 1228 (1963).
11. M. Aven and J.A. Parodi, *J. Phys. Chem. Solids*, **13**, 56 (1960).
12. A.G. Fischer, *J. Electrochem. Soc.*, **109**, 1043 (1962).
13. A.G. Fischer, *J. Electrochem. Soc.*, **110**, 733 (1963).
14. Y.Y. Chen, J.G. Duh, B.S. Chiou, and C.G. Peng, *Thin Solid Films*, **392**, 50 (2001).
15. H. Kawai, S. Kuboniwa, and T. Hoshina, *Jpn. J. Appl. Phys.*, **13**, 1593 (1974).
16. D.C. Joy, *Monte Carlo Modeling for Electron Microscopy and Microanalysis* (Oxford University Press, New York, 1995).
17. M. Savelli and J. Bounnot, in *Solar Energy Conversion: Solid-State Physics Aspects*, edited by B. O. Seraphin (Springer, Berlin, 1979), p. 228.
18. M. Savelli and J. Bounnot, in *Solar Energy Conversion: Solid-State Physics Aspects*, edited by B. O. Seraphin (Springer, Berlin, 1979), p. 213.
19. M.T.S. Nair and P.K. Nair, *Semicond. Sci. Technol.*, **4**, 191 (1989).